International Journal of Pharmaceutical Research and Development (IJPRD)
Platform for Pharmaceutical Researches & Ideas
www.ijprd.com

ANTIBACTERIAL ACTIVITY OF COPPER OXIDE NANOPARTICLES AGAINST GRAM-NEGATIVE BACTERIAL STRAIN SYNTHESIZED BY REVERSE MICELLE TECHNIQUE

Renu Rani*[1],
Harish Kumar[1], Raj Kumar Salar[2], and Sukhvinder Singh Purewal[2]

*[1]Department of Chemistry, Ch. Devi Lal University, Sirsa (Haryana) India – 125 055
[2]Department of Biotechnology, Ch. Devi Lal University, Sirsa (Haryana) India – 125 055

ABSTRACT

Monoclinic CuO nanoparticles were synthesized by reverse micelle technique. Size and morphology were characterized by using XRD, and TEM techniques. FTIR technique was used to ensure the bonding between metal and oxygen. Antibacterial activity of CuO nanoparticles were tested against bacterial strains K. pneumoniae, S. typhimurium, and E. aerogenes using the agar diffusion method. Minimum inhibitory concentration of these three gram-negative bacterial strains K. pneumoniae, S. typhimurium, and E. aerogenes were found to be 0.55, 0.15, and 0.30 µg/ml, respectively.

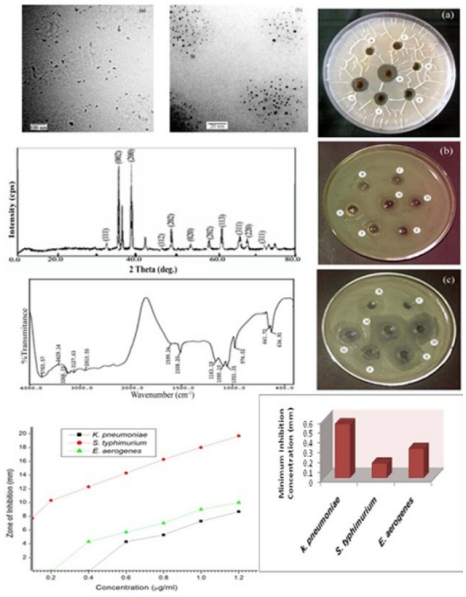

Correspondence to Author

Renu Rani

Department of Chemistry, Ch. Devi Lal University, Sirsa (Haryana) India – 125 055

Email: renuinsan777@gmail.com

Keywords : *Nanoparticles, XRD, TEM, FITR, Antibacterial activity.*

INTRODUCTION

With recent advances in nanotechnology, various types of metal and metal oxide nanoparticles with antimicrobial (microbiocidal or growth-inhibiting) activity have been synthesized[1-9]. Metal nanoparticles containing magnesium oxide[6], copper[7, 8], silver[1-5], iron[10], zinc oxide[11-13], and nickel oxide[14, 15] are exhibit antimicrobial properties.

The antimicrobial activity has been observed to vary as a function of surface area in contact with the microbe; therefore nanoparticles with large surface area ensure a broad range of reactions with the bacterial surface[16].

Compare to other methods, the reverse micelle method is one of the most promising wet chemistry synthesis approaches[17] of synthesis of metal nanoparticles. This method provides a favorable microenvironment for controlling the chemical reaction. As such the reaction rate can be easily controlled, and it is possible to obtain a narrow nanoparticle size distribution[18]. The size of the core of the reverse micelle can also be controlled by changing water to surfactant ratio[19]. Reverse micelle microemulsions are transparent, isotropic, and thermodynamically stable[20, 21].

In continuation of our earlier reported work on nickel, zinc, and silver nanoparticles[22-25], CuO nanoparticles were synthesized using microemulsion technique. Characterization of CuO nanoparticles were carried out using TEM, XRD, and FTIR. Antibacterial activity of CuO nanoparticles were also investigated against four bacterial strains.

EXPERIMENTAL:

Materials and method:

All chemicals used in experiment were of analytical grade. The stable reverse micelle microemulsion was prepared by mixing a non-ionic surfactant Triton X-100 [$(C_{14}H_{22}O(C_2H_4O)_n$] (Qualigen Chem. Pvt. Ltd.),Polyvinyl pyrollidone (PVP) (K85-95) (Merk) and 1:9 ratio of cyclohexane (Qualigen Chem. Pvt. Ltd.) and triple distilled water (conductivity less than 1×10^{-6} S cm^{-1}) (W/S ratio 5). The microemulsion was mixed rapidly with continuous stirring for five minutes. $CuSO_4.5H_2O$ (Qualigen Chem. Pvt. Ltd.) solution (0.5 M) was added drop by drop to microemulsion with continuous stirring. A sky blue colour mixture was obtained. PVP was used as a stabilizing agent. After half an hour of equilibration, 2.0 M hydrazine hydrate (Qualigen Chem. Pvt. Ltd.) solution was added drop by drop with continuous stirring at room temperature. The mixture gradually changed from sky blue to reddish brown without precipitation. The reverse micelles were broken by adding THF (Merk).

CuO nanoparticles were subsequently washed with ethanol and triple distilled water to remove residual PVP and surfactant molecules. After washing CuO nanoparticles were dried in oven at 100.0 °C for 48 hours.

Characterization techniques:

Structural and optical properties of the CuO nanoparticles were determined by using Transmission Electron Microscopy (TEM) (Hitachi: H-7500; Resolution: 2 Å), X-ray Diffraction (XRD) (Rikagu Mini-2 using CuKα1, λ = 0.15406 nm radiations), and Fourier Transform Infra- Red spectroscopy (FTIR) (Thermo-USA, FTIR-380) in the wavelength range of 400 - 4000 cm^{-1}.

Antibacterial Activity:

Bacterial strains were obtained from the Microbial Type Culture Collection (MTCC), Institute of Microbial Technology (Chandigarh). The culture media; Beef extract and Agar-agar Type-1 (Hi-Media Pvt. Ltd., Bombay), and chemicals; Peptone, Sodium Chloride (Qualigen Chemicals Pvt. Ltd., Bombay) were used for the growth of bacteria.

Antibacterial Activity in Solid Method:

Antibacterial activity of CuO nanoparticles were tested against three gram negative bacterial strains of *Klebsiella pneumoniae* (MTCC 3386) *Salmonella typhimurium* (MTCC 1253), and *Enterobacter aerogenes* (MTCC 2823) using the agar well diffusion assay method[26]. Approximately, 25.0 ml of molten and cooled nutrient agar media was poured in the sterilized petri dishes. The plates were left over night at room temperature to check for any contamination to appear. The bacterial test organism *K. pneumoniae*, *S. typhimurium*, and *E. aerogenes* were grown in nutrient broth for 24 hours at 37 °C. A 100 µl nutrient broth

culture of each bacterial organism was used to prepare bacterial lawns. Agar wells were prepared with the help of a sterilized stainless steel cork borer. Agar wells were prepared with the help of a sterilized stainless steel cork borer. The wells in each plate were loaded with 100 µl of different concentrations i.e. 0.10, 0.20, 0.40, 0.60, 0.80, 1.0 and 1.2 µg/ml of copper oxide nanoparticles.

Antibacterial Activity in Liquid Method:

A 100 µl nutrient broth culture of each bacterial organism was added to 100 ml solution of different concentrations i.e. 0.10, 0.20, 0.40, 0.60, 0.80, 1.0 and 1.2 µg/ml of copper oxide nanoparticles and incubated at 37 °C for 24 hrs. To study the bacterial concentration, the optical density values were taken at 600 nm.

RESULTS AND DISCUSSION:

Synthesis:

Copper sulfate pentahydrate contains Cu (II) in a geometry best described as distorted octahedral. Here Cu (II) is bound to four water molecules in a square-planar geometry and two oxygen atoms of sulfate ions. Due to the solvating action, $CuSO_4.5H_2O$ dissolves in water to produce the pale-blue colour $[Cu(H_2O)_6]^{2+}$ ions, in which two of the water molecules are less tightly held than the others.

Addition of $N_2H_4.H_2O$ to the aqueous solutions of copper sulphate pentahydrate results to produce the reddish brown precipitates of Cu nanoparticles inside the reverse micelle core. PVP stabilize these Cu nanoparticles. The surfactant and PVP molecules adhere to the surface of nanoparticles which serve as a protective layer to prevent the further reaction. The Cu nanoparticles are oxidized into CuO nanoparticles in the presence of atmospheric O_2 gas at 100 °C. The reaction motile of formation CuO nanoparticles can be followed as:

$$CuSO_4(aq)+N_2H_4+2H_2O(l)\rightarrow 2Cu(s)+2(N_2H_5)SO_4(aq)+O_2 \quad (1)$$

$$2Cu(s) + O_2 \rightarrow 2CuO(s) \quad (2)$$

There are two important factors that affect the exchange rate of reverse micelles in microemulsions; the dimer stability and the size of channels between the dimmers[27]. The dimer stability, which depends on the intermicellar attractive potential, determines the interdroplet transfer of reactants. On the other hand, the size of channels which depends on the rigidity of interfacial film in the microemulsion, determines the Ostwald ripening contribution[28].

Tranmission Electron Microscopy and X-Ray Diffraction Analysis:

Spherical shape of CuO nanoparticles were observed from TEM images (Figure 1a, and b). The average size of copper oxide nanoparticles was found to be 5.0 – 8.0 nm. It was indicate that surfactant molecules form a film over the surface of CuO nanoparticles which prevented the agglomeration of nanoparticles.

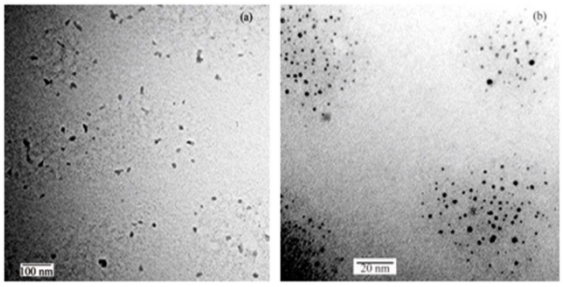

Fig. 1 TEM images of CuO nanoparticles (a, b).

XRD diffraction patterns of CuO nanoparticles are shown in Figure 2. The peaks are indexed as 33.72º (111), 35.86º (002), 39.46º (200), 46.68º (112), 49.06º (211), 53.85º (020), 58.92º (202), 62.06º (113), 66.72º (311), 67.98º (220) and 73.04º (311), respectively[29]. All diffraction peaks of sample correspond to the characteristic monoclinic structure of copper oxide with lattice

constant of a = 0.46837 nm, b = 0.34226 nm and c = 0.51288 nm. Similar peaks of copper oxide nanoparticles were reported by A. K. Lagashetty and his coworkers[30] and Fei-Fei Cao et. al.[31]. Average particle size of copper oxide nanoparticles calculated using Scherrer equation[32] was 6.0 nm respectively.

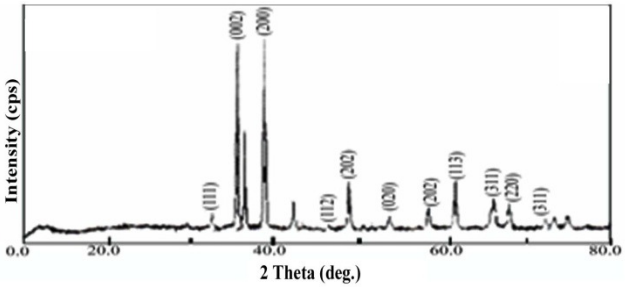

Fig. 2 XRD patterns of CuO nanoparticles.

FTIR Spectroscopy:

Figure 3 shows FTIR spectra of the nanoparticles. The peak at 3765.57 cm^{-1} may be due to O–H bond stretching assigned to H_2O present and at 1163.29 cm^{-1} may be due to O–H bond deformation assigned to the water adsorption. The peaks at 3266.33 and 3227.63 are attributed to the ≡C–H symmetrical and asymmetrical stretching modes, respectively. The peak at 2910.55 cm^{-1} due to –C–H bond stretching assigned to alkyl group. The peak at 974.02 cm^{-1} is attributed due to C–H out of plane deformation and C–O stretching assigned due to the peaks at 1090.10 and 1051.35 cm^{-1} coordinate to the metal cations[33]. The peaks at 1599 and 1508.20 cm^{-1} are correspond to the Cu–O symmetrical and asymmetrical stretching and the peaks at 641.72 and 634.92 cm^{-1} are correspond to the Cu–O deformation vibration. The metal-oxygen frequencies observed for the respective metal oxides are in close agreement with literature values[34, 35].

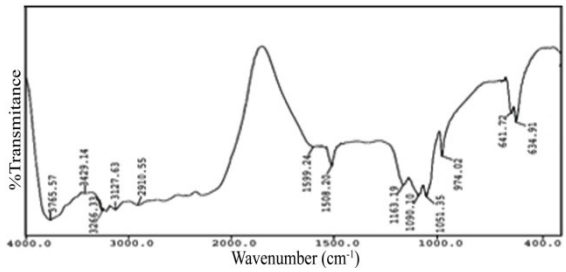

Fig. 3 FTIR spectra of CuO nanoparticles.

Antibacterial Activity:

The effect of different concentration of CuO nanoparticles like B, C, D, E, F, G, and H as 0.1, 0.2, 0.4, 0.6, 0.8, 1.0, and 1.2 µg/ml, respectively shows in Figure 4 (a, b, and c).

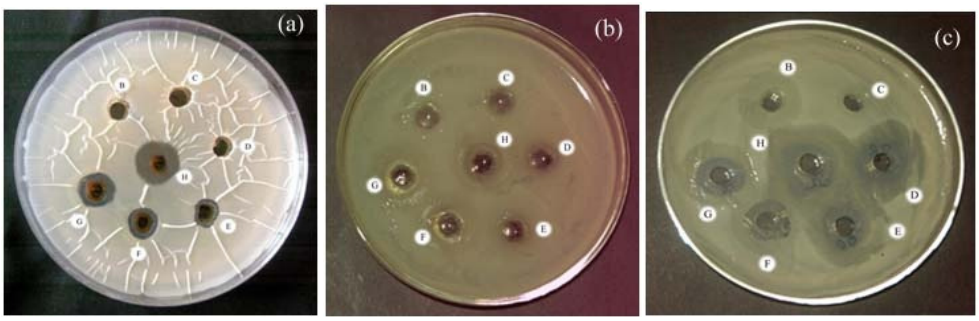

Fig. 4 Antibacterial activity of CuO nanoparticles at different concentrations against *K. pneumoniae*, *S. typhimurium*, and *E. aerogenes* as a, b, and c, respectively.

Figure 5 shows increase of the inhibition zone measurements with increase the concentration of CuO nanoparticles.

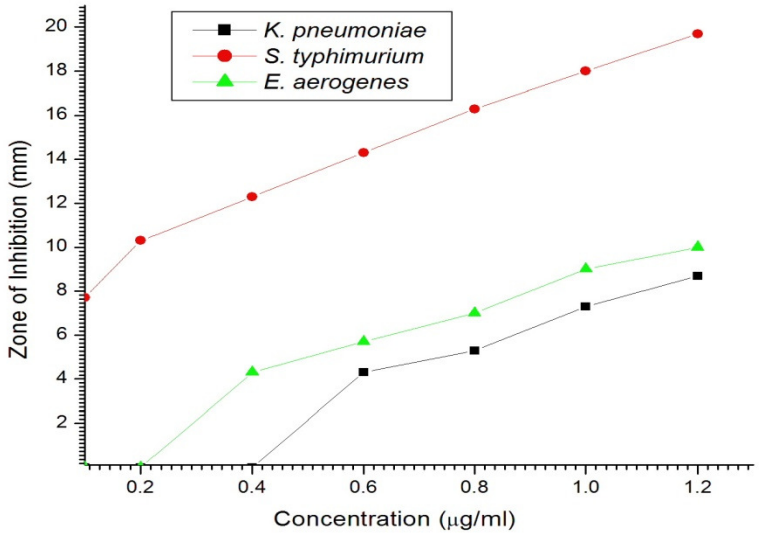

Fig. 5 Zone of inhibition (mm) of *K. pneumonia, S. typhimurium* and *E. aerogenes* at different concentration of CuO nanoparticles.

Minimum inhibition concentration (MIC) of copper oxide nanoparticles also determined on the basis of diameter of zone of inhibition as shown in Figure 6. Minimum inhibitory concentration of these three gram-negative bacterial strains *K. pneumoniae*, *S. typhimurium*, and *E. aerogenes* were found to be 0.55, 0.15, and 0.30 µg/ml, respectively.

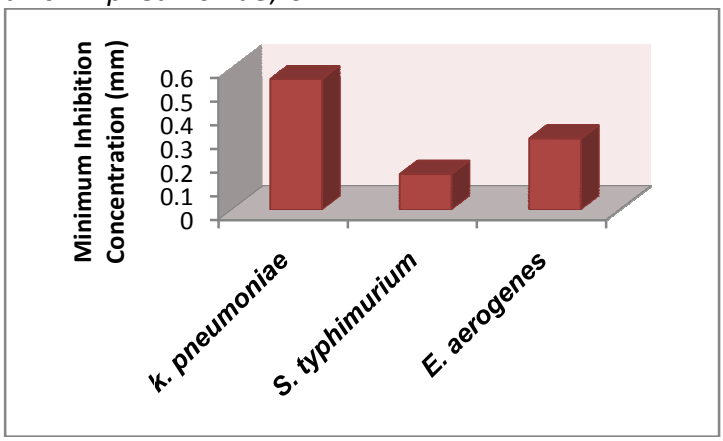

Fig. 6 MIC (mm) of CuO nanoparticles against *K. pneumoniae*, *S. typhimurium*, and *E. aerogenes.*

CONCLUSION

CuO nanoparticles were synthesized by microemulsion technique. TEM images indicate spherical shape of CuO nanoparticles of 5.0 – 8.0 nm in diameter. It is suggests that surfactant molecules form a film over the surface of CuO nanoparticles which prevented the agglomeration of nanoparticles. Monoclinic structure of CuO nanoparticles with average particles size of 6.0 nm in W/S ratio of 5.0 was observed by XRD. FTIR spectra confirm the presence of metal oxygen bond. Antibacterial characterization has been demonstrated against three gram-negative bacterial strains i.e. *K. pneumoniae*, *S.*

typhimurium, and *E. aerogenes* using the agar well diffusion assay method. CuO nanoparticles adhered to the cell wall of bacteria and penetrated through the cell membrane. This resulted into inhibition of bacterial cell growth and multiplication, which finally leads to cell lysis.

REFERENCES:

1. Alt V, Bechert T, Steinrcke P, Wagener M, Seidel P, Dingeldein E, Domann U, Schnettler R, An in vitro assessment of the antibacterial properties and cytotoxicity of nanoparticulate silver bone cement, Biomat Biomater, 25, 2004, 4383-4391.
2. Furno F, Morley KS, Wong B, Sharp BL, Arnold PL, Howdle SM, Bayston R, Brown PD, Winship PD, Reid H, Silver nanoparticles and polymeric medical devices: a newapproach to prevention of infection, J Antimicrob Chemother, 54, 2004,1019- 1024.
3. Jeong SH, Yeo SY, Yi SC, The effect of filler particle size on the antibacterial properties of compounded polymer/silver fibers, J Mater Sci, 40, 2005, 5407-5411.
4. Chou WL, Yu DG, Yang MC, The preparation and characterization of silver-loading cellulose acetate hollow fiber membrane for water treatment, Poly Adv Technol, 16, 2005, 600-607.
5. Sambhy V, MacBride MM, Peterson BR, Sen A, Silver bromidenanoparticle/polymer composites: dual action tunable antimicrobial materials, J Am Chem Soc, 128, 2006, 9798-9808.
6. Stoimenov PK, Klinger RL, Marchin GL, Klabunde K, Metal oxide nanoparticles as bactericidal agents, Lang, 18, 2002, 6679-6686.
7. Hsiao MT, Chen SF, Shieh DB, Yeh CS, One-pot synthesis of hollow Au_3Cu_1 spherical- like and biomineral botallackite Cu-2(OH)(3)Cl flowerlike architectures exhibiting antimicrobial activity, J Phys Chem B, 110, 2006, 205-210.
8. Theivasanthi T, Alagar M, Studies of copper nanoparticles effects on micro-Organisms, Annals Bio Res, 2(3), 2011, 368-373.
9. Morones JR, Elechiguerra JL, Camacho A, Holt K, Kouri JB, Ramírez JT, Yacaman MJ, The bactericidal effect of silver nanoparticles, Nanotechnol, 16, 2005, 2346-2353.
10. Lee C, Kim Y, Lee WI, Nelson KL, Yoon J, Sedlak DL, Bactericidal effect of zero-valence iron nanoparticles on *Escherichia coli*, Environ Sci Technol, 42(13), 2008, 4927-4933.
11. Zvekic D, Srdic VV, Karaman MA, Matavulj MN, Antimicrobial properties of ZnO nanoparticles incorporated in polyurethane varnish, Proc Appl Cer, 5(1), 2011, 41-45.
12. Rajendran R, BalaKumar C, Ahammed HAM, Jayakumar S, Vaideki K, Rajesh EM, Use of zinc oxide nanoparticles for production of antimicrobial textiles, Int J Engg Sci Technol, 2(1), 2010, 202-208.
13. Gondal MA, Dastageer MA, Khalil A, Hayat K, Yamani ZH, Nanostructured ZnO synthesis and its application for effective disinfection *Escherichia coli* micro organism in water, J Nanopart Res, 133, 2011, 423-430.
14. Wangsaprom K, Maensiri S, Synthesis structural characterization of nickel oxide nanoparticles synthesized by polymerized complexed (PC) method, Proceed in 3rd Int Nanoelec Conf 2010, 1044-1045.
15. Kavitha T, Yuvaraj H, A facile approach to the synthesis of high-quality NiO nanorods: electrochemical and antibacterial properties, J Mater Chem, 21, 2011, 15686-15691.
16. Holister P, Weener JW, Vas CR, Harper T, Nanoparticles-Technology white papers, 3, Cientific Ltd, London, 2003.
17. Arriagada FJ, Osseo-Asare K, Synthesis of nanosize silica in a nonionic water-in-oil microemulsion: Effects of the water /surfactant molar ration and ammonia concentration, J Coll Inter Sci, 211, 1999, 210-220.
18. Bae DS, Jungkim E, Bang JH,Kim SW, Han KS, Kyulee J, Kim BI, Adair JH, Synthesis and characterization of silver nanoparticles by a reverse micelle process, J Met Mater-Int, 11(4), 2005,291-294.
19. Ganguli AK, Vaidya S, Ahmad T, Synthesis of nanocrystalline materials through reverse

micelles: A versatile methodology for synthesis of complex metal oxides, J. Bull. Mater. Sci., 2008, 31(3), 415-419.
20. Bae DS, Park SW, Han KS, Adai JH, Syntheisis of Ag/SiO_2 nanosize particles by reverse micelle and sol-gel processing, J Met Mater.-Int, 7, 2001, 399-402.
21. Pileni MP, Structure and reactivity in reverse micelles, Elsevier, Amsterdam, New York, 1989.
22. Kumar H, Rani R, Salar RK, 2010, Reverse micellar synthesis, characterization and antibacterial study of nickel nanoparticles, Europ Conf Adv Cont-Chem Engg & Mech.Engg, 2010, 88-94.
23. Kumar H, Rani R, Salar RK, Synthesis of nickel hydroxide nanoparticles by reverse micelle method and its antibacterial activity, Res J Chem Sci, 1(9), 201,1-7.
24. Kumar H, Rani R, Structural and optical characterization of ZnO nanoparticles synthesized by microemulsion route, Int Let Chem Phys Astro, 14, 2013, 26-36.
25. Kumar H, Rani R, Structural characterization of silver nanoparticles synthesized by microemulsion route, Int J Engg Inno Technol, 3, 2013, 344-348.
26. Perez C, Paul M, Bazerque P, Antibiotic assay by agar well diffusion method, Acta Bio Med Exp, 15, 1990, 113-115.
27. Quintillán S, Tojo C, Blanco MC, López-Quintela M A, Effects of the intermicellar exchange on the size control of nanoparticles synthesized in microemulsions, Langmiur, 17, 200, 17, 7251-7254.
28. Dodoo-Arhin D, Leoni M, Scardi P, Microemulsion Synthesis of Copper Oxide Nanorod-Like Structures, Mole Crys Liq Crys, 555, 2012, 17-31.
29. Joint Committee on powder diffraction standards (2000) Diffraction data file, No 05–0661.
30. Lagashetty A, Havanoor V, Basavaraja S, Balaji SD, Venkatarman A, Microwave- assisted route for synthesis of nanosized metal oxides, Sci Tech Adv Mat, 8(6), 2007, 484-493.
31. Cao F-F, Xin S, Guo YG, Wan L-J, Wet chemical synthesis of Cu/TiO2 nanocomposites with integrated nano-current-collectors as high-rate anode materials in lithium-ion batteries, Phys Chem Chem Phys, 13, 2011, 2014-2020.
32. Culity BD, Elements of X-ray diffraction, second ed, Addison-Wesley, USA, 1987.
33. Bernson A, Lindgren J, Huang W, Frech R, Coordination and conformation inPEO, PEGm and PEG systems containing lithium or lanthanum triflate, Polymer, 36(23), 1995, 4471-4478.
34. Rao CNR, Chemical Applications of Infrared spectroscopy, Academic Press, New York and London, 1963.
35. Markova-Deneva I, Infrared spectroscopy investigation of metallic nanoparticles based on copper, cobalt and nickel synthesized through borohydride reduction method, J Univ Chem Tech Metal, 45(4), 2010, 351-378.

*****